

Preparation of Nonequilibrium Materials by Mechanical Alloying[†]

Z. Q. Hu H. F. Zhang Z. G. Liu L. L. Ye
G. J. Fan H. W. Sheng^{*}

State Key Laboratory of Rapidly Solidified Nonequilibrium Alloys Institute of Metal Research,
Shenyang, 110015, China

Abstract: During the recent years, mechanical alloying/ball milling was widely employed to synthesize the new kinds of nonequilibrium materials, namely, by means of solid state reactions to form materials with metastable structures. In the process of ball milling, starting powders are subjected to the repeated fracture and cold welding that lead to the accumulation of internal defects and stored energy. Consequently, the microstructures of the milled powders are refined.

Abrupt temperature rise, amorphization, local melting and formation of metastable phase have been observed. Mechanical alloying also has a remarkable influence on the microstructure and mechanical properties. Some differences have also been found in the formation products produced by mechanical alloying and rapid quenching, for example, on melting point depression hardenability and thermal stability.

Key words: Nonequilibrium material; Mechanical alloying; Metastable phase

1 Introduction

The ball milling technique was originally developed to manufacture oxide–dispersion–strengthened (ODS) alloys for high–temperature applications performed at INCO Research Laboratory in the early 1960s^[1]. In 1983, Koch and coworkers^[2] discovered that, during milling of elemental niobium and nickel powders in a Spex 8000mill, the final product was found to be an amorphous

[†] 本文原载于《Proc. of 1st Int. Conf. on Advanced Materials Processing.》, 2000, 1~12.

^{*} Editors: D. L. Zhang, K. L. Pickering, X. Y. Xiong; Institute of Materials Engineering Australasia © 2000.

structure. This was demonstrated by the disappearance of the crystalline reflections in X-ray diffraction and appearance of a broad peak, characteristic of an amorphous structure. After this discovery by Koch and coworkers, further investigations of amorphization induced by ball milling were carried out by Schwarz et al.^[3] in the Ni-Ti binary system, Hellstern and Schultz^[4] for a number of transition-metal-zirconium systems, and by Weeber et al.^[5] for the Ni-Zr system. In the later investigation, it was shown that nickel almost loses its magnetic moment after long milling times, which clearly demonstrated the mixing on an atomic scale by ball milling. Since a true alloying process rather than solely refinement of microstructures occurred during ball milling, this process is thus termed “mechanical alloying”(MA).

Since these pioneer researches on mechanical alloying, research activities on the formation and properties of metastable phases such as amorphous phase using mechanical alloying have gathered world wide attention in the field of the materials science. MA has been attracting enthusiastic attentions among researchers. Besides amorphization of the mixed elemental powders by MA, it was found that MA can also be used to synthesize the extended solid solutions that are otherwise immiscible, nanophase materials, et al.^[6], which is in close analogy with other nonequilibrium processing methods such as rapid quenching. In addition, it was shown that ball milling can cause the loss of long range order and amorphization of the intermetallic compounds. Yermokov et al.^[7] reported that intermetallic compounds in Y-Co system can be amorphized after ball milling. After that, Schwarz and Koch^[8] reported that the amorphous Ni-Ti and Ni-Nb alloys can be obtained by milling of the crystalline NiTi₂ and Ni₄₅Nb₅₅ intermetallic compounds. In contrast to the mechanical alloying of mixture of elemental powders, where materials transfer occurs. The milling of the prealloyed intermetallic compounds does not involve the materials transfer and thus is termed “mechanical milling” (MM).

In the following sections, a brief review will be made to summarize the research activities in the field of mechanical alloying in the State Key Laboratory of Rapidly Solidified Nonequilibrium Alloys.

2 Characteristics of Mechanical Alloying

2.1 Abrupt Temperature Rise

Elemental Al, Ti, and C powders with average particle sizes of $15\mu\text{m}$, $74\mu\text{m}$, and $250\mu\text{m}$, respectively, and with purity of 99.9at% mixed at the composition of Ti+C+25wt% Al with a batch of 10g were milled in a domestic-made high energy ball mill. The powders and stainless steel balls were sealed in a stainless steel container under Ar atmosphere, with a ball-to-powder weight ratio of 10:1. During milling, the temperature of the milling container was monitored with a thermocouple attached to its outer side. The temperature was recorded by an X-Y recorder.^[9]

Figure 1(a) shows the recorded temperature profile of the outer side of the container during mechanical alloying Ti-C-25wt% Al. A steady-state temperature of 30°C was attained after milling for around 200min, and a temperature spike of the container was observed after milling for 210min. The rapid temperature rise indicated a large amount to heat dissipation due to the exothermal reaction in the vial occurred in a short time. The corresponding product milling for 180min and 210min were analyzed by XRD and shown in Fig.2. No new phase was detected after milling for 180min, except the elemental peaks, while TiC and TiAl phases with sharp and intensive diffraction peaks were obtained after the combustion reaction. The XRD results coincided with the record of the temperature change. The lattice parameter of TiC is precisely measured to be 0.4326nm using its (113) peak.

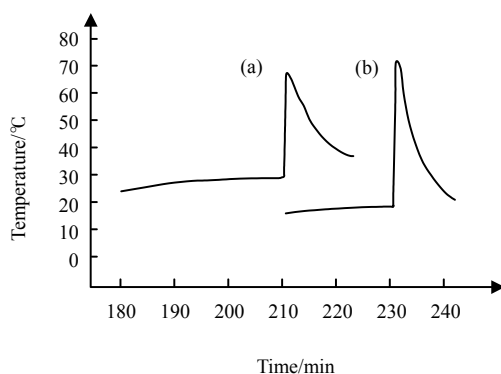


Fig. 1 In-situ thermal analysis of
(a)Ti-C-25wt% Al; (b)Ti₅₉C₄₁^[9]

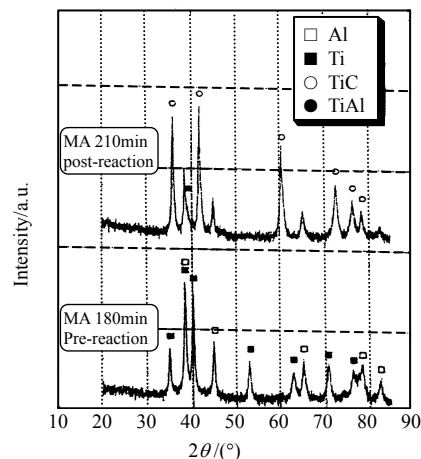


Fig. 2 XRD patterns of Ti-C-25wt% Al
after milling (bottom) 180min and
(top)210min^[9]

Based on the information provided by in situ thermal analysis, the reaction

temperature is estimated to be 1677K, which is in good agreement with the value of the adiabatic temperature of 1700K. It is considered that the formation reaction of Ti-C, which ignited by the heavy collisions of milling balls, induced the following reaction between Ti and Al at high temperature.^[9]

Similar phenomenon was also observed in the MA reaction between Si and PbO powders^[10] in the synthesis of NbSi₂ by mechanical alloying elemental Nb and Si powders^[11] and of TiC or NbC from Ti, Nb and C powders^[12,13] which can be proved by Fig.3.

Fig.4 shows the XRD patterns of the milling of Ni and Al powders and the formation of NiAl abruptly after 88min mechanical alloying^[14]. On the contrary, if Fe and Al powders were milled, no abrupt temperature change happened due to the low heat of formation of FeAl(6000 cal/(g · atom)) as compared to that of NiAl(14000cal/(g · atom))^[15]. The addition of 5 at % Ti prolongs the milling time of alloy for 21min prior to the explosive reaction.^[16]

2.2 Local Melting

The Ni, Ti and graphite powders, with nominal purities of 99.0%, 99.9%, and 99.9at% and average particle sizes of 74 μm, 74 μm, and 250 μm, respectively, mixed at composition of Ni₂₀Ti₅₀C₃₀ and Ni₅₀Ti₃₀C₂₀, were milled in a planetary ball mill. The ball-to-powder weight ratio is 40:1. Balls and powders were sealed in Ar atmosphere during the entire milling process.^[17] The morphologies of the agglomerates and powders also exhibit large differences (Fig5(a), (b)). The powder samples are granular with particle sizes from 3~7μm. However, the agglomerates show an appearance similar to the solidification of running liquid, and no sharp end and edge was observed. This is evidence of melting and solidification. The SEM observation (Fig5(c)) of the polished section of the agglomerate sample shows that the TiC particles appear spherical and monodispersed, which indicates that TiC particles was surrounded by liquid during milling, and the spherical appearance of TiC formed to decrease the surface energies.

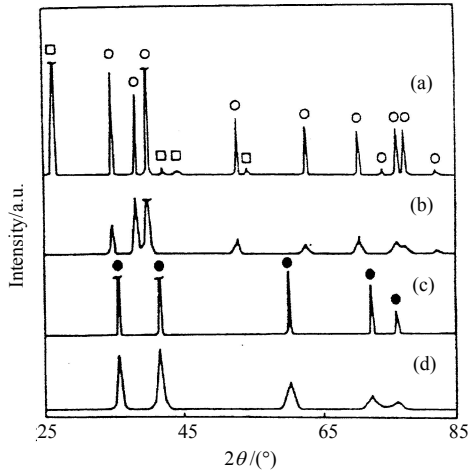


Fig. 3 XRD patterns of $Ti_{50}C_{50}$ powders after milling

(a)0h; (b)3h; (c)186min; (d)15h
 \circ Ti; \square C; \bullet TiC^[12]

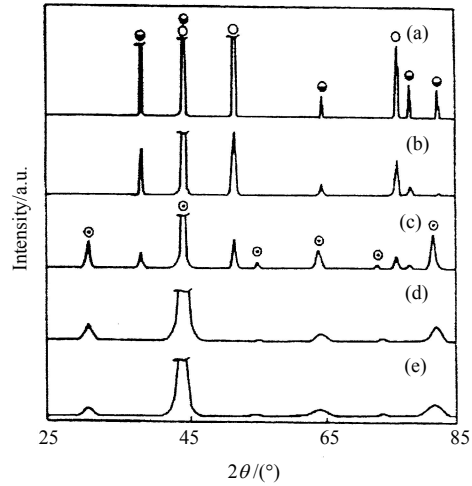


Fig. 4 XRD patterns of $Ni_{50}Al_{50}$ after milling for

(a)0h (as-mixed); (b)1h; (c)88min (1min after reaction);
 (d)5h; (e)30h
 \circ Ni; \bullet Al; \odot NiAl^[14]

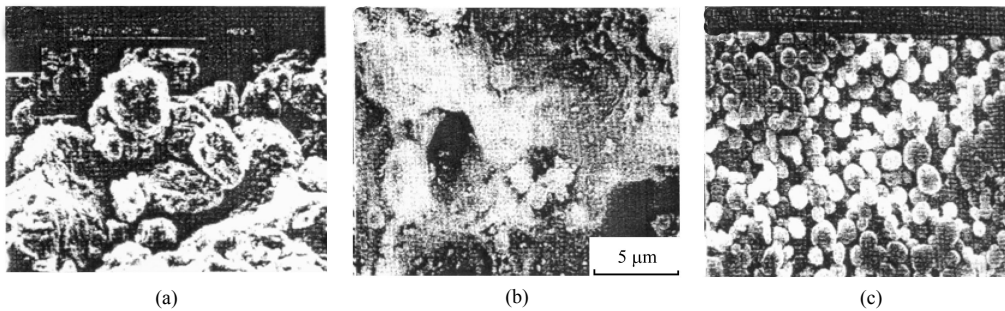


Fig. 5 Scanning Electron Micrograph of $Ni_{20}Ti_{50}C_{30}$ Powder Mixture Milled for 215min

(a) powders; (b) agglomerates; (c) SEM of (b)^[17]

The ignition of the combustion reaction is the large heat releasing from the initial formation of TiC through heavy collisions of milling balls, which supplies the ample condition for the reaction, while the addition of Ni provides the essential condition for the reaction self-sustained. It is reasonable to induce that the reaction mechanism of TiC both in $Ni_{20}Ti_{50}C_{30}$ and $Ni_{50}Ti_{30}C_{20}$ is mainly controlled by the diffusion of elemental C through solid Ti and TiC.

Dispersions of nanometer-sized In particles embedded in an Al matrix(10wt% In) have been synthesized by ball milling of a mixture of Al and In powders. It was found that In and Al are pure components immiscible with each other, with

nanometer-sized In particles dispersively embedded in the Al matrix. The calorimetric measurements indicate that the three characteristic melting temperatures, including starting temperature T_s , onset temperature T_o and peak temperature T_p , as well as the melting enthalpy of the In nanoparticles decrease with increasing milling time, or refinement of the In particles. Compared to its bulk melting temperature, a melting point depression of 13.4K was observed when the mean grain size of In is 15nm, and the melting point depression of In nanoparticles is proportional to the reciprocal of the mean grain size.^[18] By integrating the area under the endothermal peak, we obtain the released heat, L_m , for the melting of In particles per gram of the Al/In sample. With an increasing milling time, or a refinement of the In, L_m decreases monotonically. After milling for 300h, the released heat for In melting is depressed by 61% compared to that of the unmilled Al/In sample. The measured values are listed in Table 1.

Metastable $Fe_{100-x} Al_x$ alloys have been formed by ball milling of elemental Fe and Al powders: supersaturated body-centered-cubic solid solution for $x \leq 70$, and an amorphous phase for $x > 70$. Quantitative X-ray-diffraction measurements show that the total root-mean-square displacement (rms) and the static rms in the $Fe_{100-x} Al_x$ solid solutions increase significantly with increasing Al content (Fig.6). The total rms at the instability point, however, reaches only 6.8% of the nearestneighbor distance and is far below the critical value predicted by the Lindemann melting criterion, suggesting that it is not applicable for the solid-state amorphization. Instead, the Debye temperature of the supersaturated $Fe_{100-x} Al_x$ alloys was observed to drop by ~ 22% at the point of amorphization, implying a corresponding softening in the average shear modulus of ~ 40%, which agrees with the microhardness measurements (Fig.7). These results strongly support the empirical elastic instability criterion for the solid-state amorphization process.^[19]

Table 1 Melting temperature and grain size versus milling time^[18]

Milling Time/h	d/nm	T_s /K	T_o /K	T_p /K	ΔT_o /K	L_m (J/g)
Unmilled/0h	...	428.4	429.0	429.7	0	2.84
3	75	431.7	427.7	429.6	1.5	2.57
10	34	416.0	422.5	426.7	6.5	1.95
30	30	415.0	422.2	426.8	6.8	1.79

70	24	412.4	420.1	425.7	8.9	1.70
100	21	409.0	419.4	425.4	9.6	1.60
200	18	408.1	416.9	423.9	12.1	1.25
300	15	408.0	415.6	424.2	13.4	1.10

The partial fusion of In particles was also observed in the light energy ball milling of Al and In powders^[20] as well as Ni, Ti, C powders.^[21]

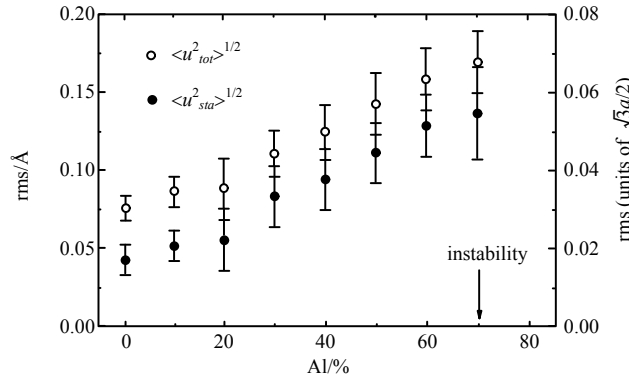


Fig. 6 Total and static root-mean-square displacements versus Al concentration^[19]

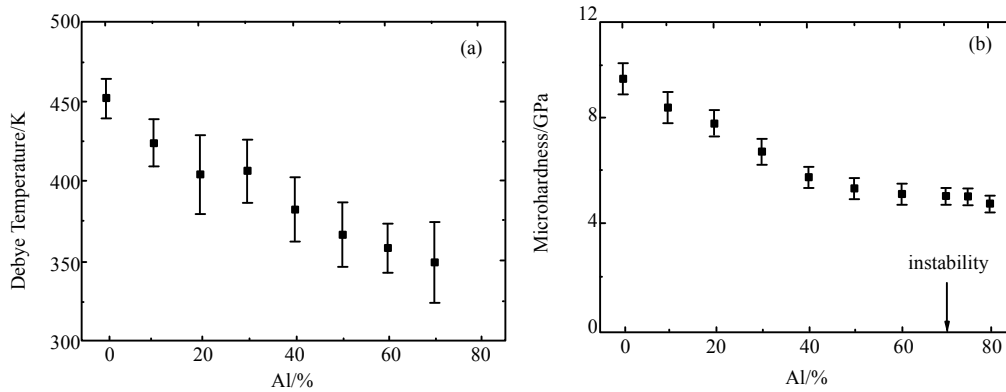


Fig. 7 Debye temperature plotted against Al concentration for Fe–Al compositions derived from x-ray-diffraction measurements(a); Variation of the microhardness for as-prepared Fe–Al solid solution with different Al concentrations, indirectly showing the elastic modulus softening(b)^[19]

2.3 Amorphization

The most unusual was the MA of $\text{Ni}_{50}\text{Al}_{25}\text{Ti}_{25}$. Mechanical milling to 30h resulted in the formation of an amorphous-like product from the disordered β phase NiAl(Ti) (Fig.8). The structural evolution of the initial milling stage was similar to that of $\text{Ni}_{50}\text{Al}_{30}\text{Ti}_{20}$. Also, a much disordered β NiAl(Ti) formed on milling to 5h, but excessive milling induced the disappearance of (100) and (200) peaks of the β phase and the broad diffused peak at $2\theta = 44.4$ (and at $2\theta = 81$, which is almost invisible), indicating the appearance of an amorphous phase. It is

suggested that the β phase NiAl(Ti) formed by milling Ni₅₀Al₂₅Ti₂₅ became disordered more easily, and transformed into an amorphous phase as a result of the addition of a large amount of Ti, which lowered the energy threshold of formation of the amorphous phase.^[14]

Structural changes occurring in the crystalline element selenium upon high-energy ball milling has been also studied. Milling experiments have been performed at the ambient temperature and at a cryogenic temperature of -100°C , respectively. The final milling products under both conditions were found to be a fully amorphous phase after several hours of mechanical milling, that indicates during cryogenic-temperature milling amorphization procedure is faster than that at ambient temperature, as shown in Fig.9. Our experimental results suggest that amorphization of the crystalline element selenium is driven by defects created by frequent mechanical deformation.^[22]

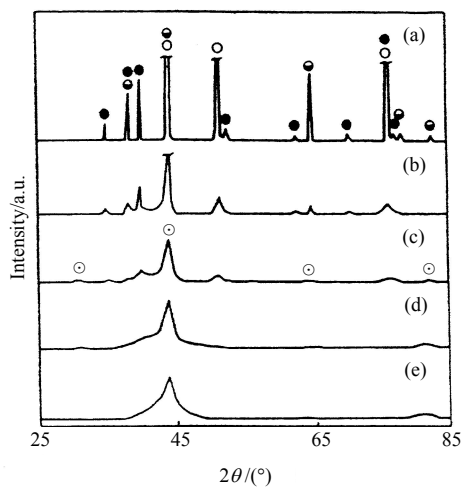


Fig. 8 XRD patterns of Ni₅₀Al₂₅Ti₂₅ after milling (a) 0h(as- mixed); (b)3h; (c)5h; (d)10h; (e)30h
○Ni; ◐Al; ●Ti; ⊙NiAl(Ti)^[14]

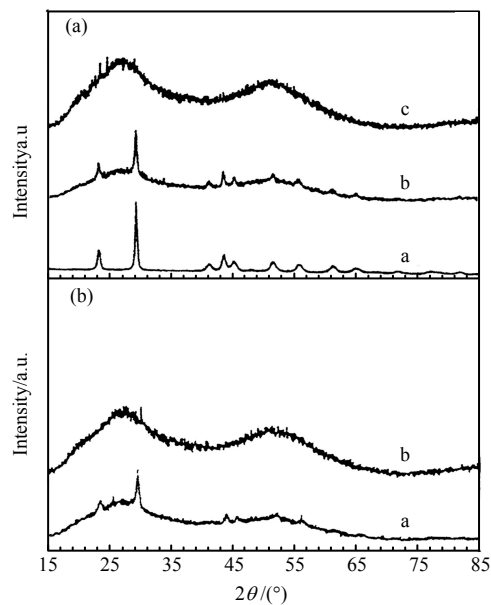


Fig. 9 XRD patterns for the element selenium^[22]
a–after (a) 0h, (b) 2h and (c) 5h of ambient-temperature milling
b– after (a) 1h and (b) 2h of cryogenic-temperature milling

Mechanical alloying (MA) of elemental powder mixture of Fe₅₀Nb₃₅C₁₅, Fe₆₀Nb₃₀C₁₀ and Fe₅₀Nb₄₀C₁₀ was performed using a high energy ball mill. In the MA

processing, ball milling first leads to a Fe–Nb–C amorphous phase and nanocrystalline NbC. Further milling results in the formation of a nanocrystalline solid solution of Fe(Nb, C) and nanocrystalline NbC in $\text{Fe}_{50}\text{Nb}_{35}\text{C}_{15}$ and $\text{Fe}_{60}\text{Nb}_{30}\text{C}_{10}$, while the final product for $\text{Fe}_{50}\text{Nb}_{40}\text{C}_{10}$ is a mixture of amorphous Fe–Nb–C and nanocrystalline NbC.^[23]

3 Influence on Microstructures

3.1 Formation of metastable phases

Recently, high energy ball milling has been used as a tool to synthesize metastable phases, e.g. supersaturated solid solution^[24], amorphous alloys^[25], nanocrystalline materials^[26,27], and quasicrystalline materials. It is a nonequilibrium process in which external energies are introduced by frequent mechanical collisions acting on a mixture of elemental powders or intermetallic compound powders.

It will be shown that the first stage of mechanical alloying an Al–Ti powder blend leads to the formation of the ordered $\text{Ll}_2\text{–Al}_3\text{Ti}$ compound at Al/Ti interfaces. The ordered $\text{Ll}_2\text{–Al}_3\text{Ti}$ compound can be partially disordered at the final stage of ball milling and a diffusional process may simultaneously happen incorporation Al or Ti into the partially disordered compound. These two processes are concurrently responsible for the formation of the supersaturated solid solution. However, partial Ll_2 ordering still may exist in the solid solution due to the incompleteness of the disordering process.^[28]

A mixture of amorphous phase and microcrystalline $\beta\text{–Ni(Al, Ti)}$ compound has been synthesized by mechanically alloying the $\text{Ni}_{50}\text{Al}_{25}\text{Ti}_{25}$ elemental powder mixtures in a high energy ball mill. It has been found that titanium plays a dominant role in this process. There exist two types of transformations of amorphous-like $\text{Ni}_{50}\text{Al}_{25}\text{Ti}_{25}$ upon heating: first, the amorphous-like alloy transforms into a disordered Ni_2AlTi compound (bcc structure) at 345~445 °C, and then into an ordered Ni_2AlTi compound at 554~626 °C. It is suggested that at the low-temperature transition, the Ni atoms locate in the corners of the bcc lattice, but the cubic centers are occupied randomly by Al and Ti atoms. When the temperature rises to 554 °C, a long-range ordering transition occurs, resulting in the formation of ordered Ni_2AlTi . The ordering energy of Ni_2AlTi has been measured as 4.35 kJ/mol. After annealing at 650 °C for 10 min, the bcc phase

transformed into ordered Ni_2AlTi , and all the diffraction peaks of the ordered Ni_2AlTi compound became visible.^[29]

For mechanically alloyed $\text{Al}_{67}\text{Ti}_{25}\text{M}_8$ ($\text{M}=\text{Cr}, \text{Zr}, \text{Cu}$), the addition of Cr and Zr can form nanocrystalline ordered $\text{Li}_2\text{-Al}_3\text{TiM}$ compounds after 40h of milling. Subsequent annealing in the differential scanning calorimeter causes a grain growth process of the nanocrystallites. With the addition of Cu, the final product was nanocrystalline disordered $\text{Al}(\text{Ti},\text{Cu})$ solid solution.^[30]

Supersaturated nanocrystalline $\text{Al}_{100-x}\text{Ti}_x$ alloys were mechanically alloyed in a planetary ball mill. For alloys with $x=5$ and 10, a supersaturated solid solution $\text{Al}(\text{Ti})$ and a fcc phase coexist, while a single supersaturated solid solution $\text{Al}(\text{Ti})$ was obtained during mechanical alloying for $x=15$ and 35. With increasing Ti content, from 5% to 35%, the grain size of the $\text{Al}(\text{Ti})$ solid solution decreased from 40 to 10nm.^[31,32]

3.2 Influence on lattice constant

The sequence of structural evolution by ball milling the polycrystalline $\text{Fe}_{80}\text{B}_{20}$ alloy was studied. It was found that ball milling polycrystalline $\text{Fe}_{80}\text{B}_{20}$ alloy results in a continuous refinement of the grain size to about 13nm. Fig.10 shows that the axial ratio c/a for the Fe_2B phase decreases whereas the unit cell expands with increasing milling time. These results indicate that chemical disordering was introduced during the mechanical deformation.^[33]

The influence on lattice constant can also be observed on Ti-Al ^[34] and Ti-C ^[35] by the variation of alloying amounts.

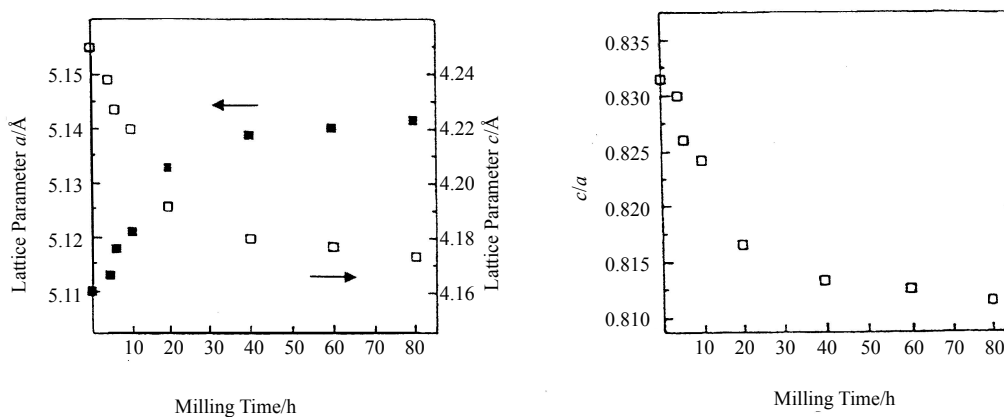


Fig. 10 Variation of Axial Ratio c/a for the Tetragonal Structured Fe_2B Phase with Milling Time^[33]

3.3 Influence on mechanical properties

The mixture of pure nickel and aluminum powders in the composition of $\text{Ni}_{50}\text{Al}_{50}$ was subjected to high energy ball milling to 30h that resulted in the

formation of a nanocrystalline NiAl with a grain size of about 10nm. The as-milled NiAl powder was hot-pressed and the compact with a density of 90% was obtained. It was showed that heating to 900 °C and holding for more than 2h failed to induce the coarsening of the fine nanocrystal in the material, the tendency of grain growth was weak.^[36]

Compression test shows that the strengths at room temperature and intermediate temperature (500 °C) are largely improved to be 1094MPa and 700MPa, and the yield strengths, 540MPa and 480MPa, respectively, as compared to the yield strength of 303MPa of a cast NiAl. It is mainly attributed to the fine grain of NiAl of 30nm. The compressive ductility at room temperature is improved to 7% from 2.8% of the cast NiAl.^[36]

3.4 Proposed mechanisms

Up to date, two kinds of reaction mechanism have been accepted in MA: (a) the colliding balls undergo severe plastic deformation, causing the flattened particles contact with clean surface, and alloys form through gradual diffusion of thin layers, and (b) the alloys form through a reaction taking place within a short time period with liberation of large heat after certain milling time, which is self-propagating high-temperature synthesis(SHS) or self-sustained reaction during mechanical alloying, and it is suggested that mechanical impact plays an important role in igniting the reaction.^[37]

Two different reaction mechanisms for $Ti_{50}C_{50}$ and $Ti_{33}B_{67}$ have also been observed respectively during milling in a planetary ball mill. It is shown that a gradual reaction occurred during milling $Ti_{50}C_{50}$, while a self-sustained reaction was obtained during milling $Ti_{33}B_{67}$ under the same milling condition. Compared with the results of milling $Ti_{50}C_{50}$ in Spex mill, the difference in mechanism is suggested to be caused by the effect of plastic deformation on the changes of fine grains and internal strain during milling and the different formation heat of TiC and TiB_2 , which is the driving force for the reactions.^[37]

A melt-spun metallic $Fe_{80}B_{20}$ glass was subjected to high-energy ball milling. It was found that the metallic glass may relax towards a low energetic configuration by mechanical milling, leading to a reduction of the heat release associated with crystallization of the amorphous phase and an increase of the average hyperfine field as well as of the Curie temperature(Table 2). These results can be attributed to the occurrence of a strong short-range order in the amorphous state. Our

experimental observations suggest that mechanical milling may induce structural relaxation in the amorphous $\text{Fe}_{80}\text{B}_{20}$ alloy.^[38]

Table 2 Variation of the heat Release ΔH , average hyperfine field H_{mean} and Curie temperature T_c for the amorphous $\text{Fe}_{80}\text{B}_{20}$ alloy with milling time^[38]

Millig Time/h	ΔH /(cal/g)	H_{mean} /kOe	T_c /K
0	128.3	243.7	682.2
0.5	128.1	245.4	684.0
1	126.1	251.8	682.4
1.5	122.7	258.4	683.8
2	124.6	264.1	687.7
2.5	123.0	265.2	688.8

4 Comparison of Nonequilibrium Materials Produced by MA and RQ

4.1 Melting point

Nanometer-sized In particles(5~45nm) embedded in the Al matrix were prepared by using melt-spinning and ball-milling techniques. Different crystallographic orientationships between In nanoparticles and the Al matrix were constructed by these two approaches. Melting behavior of the In particles were investigated by means of differential scanning calorimetry(DSC). It was found that the epitaxially oriented In nanoparticles(with the Al matrix) in the melt-spun sample were superheated to about 0~38 °C, whereas the randomly oriented In particles in the ball-milled sample melted below its equilibrium melting point by about 0~22 °C. We suggest that melting temperature of In nanoparticles can be either enhanced or depressed, depending on the epitaxy between In and the Al matrix (Fig. 11 and Table 3).^[39]

Dispersions of nanometer-sized Pb particles embedded in an Al matrix (10wt% Pb) have been synthesized by ball milling. It was found that the microstructure of Pb/Al mixture was refined with increasing milling time, resulting in nanometer-sized Pb particles homogeneously embedded in the Al matrix. The melting and freezing behaviors of the Pb particles were investigated by means of DSC. Calorimetry measurements indicated that both melting and freezing points of the Pb nanoparticles were depressed in comparison to the bulk Pb, which were

approximately proportional to the inverse particle size of Pb.^[42]

Table 3 The onset (T_o) and peak (T_p) temperatures of melting of In in the In/Al sample under different conditions(The change in the melting point with respect to the onset of the melting of the “bulk” In in as-cast In/Al, $\Delta T = T_o - T_m$ is also shown^[39-41])

Sample		Peak1			Peak2		
		$T_{o1}/^{\circ}\text{C}$	$T_{p1}/^{\circ}\text{C}$	$\Delta T / ^{\circ}\text{C}$	$T_{o2}/^{\circ}\text{C}$	$T_{p2}/^{\circ}\text{C}$	$\Delta T / ^{\circ}\text{C}$
Melt-spun(5~40nm)	1 st	155.9	163.0	-0.3	165.2	175.8	+9.0
	2 nd	156.2	161.5	0	166.8	174.3	+10.6
Ball-milled(5~45nm)	1 st	139.0	149.1	-17.2
	2 nd	139.7	152.4	-16.5
As-cast		156.0	156.7	0

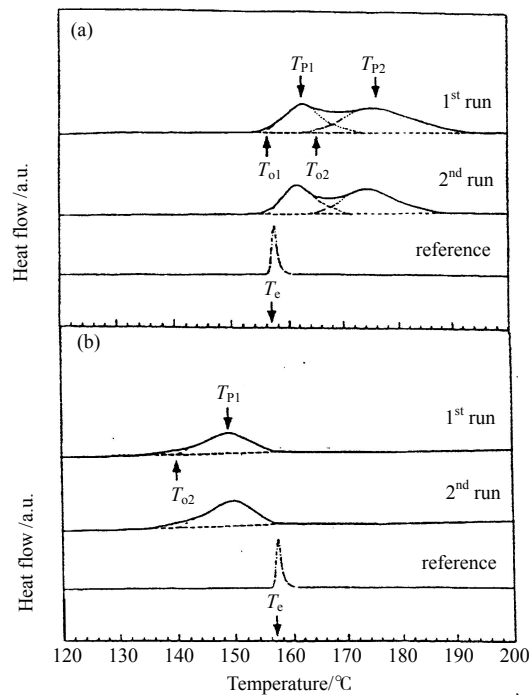


Fig. 11 DSC traces of melting endotherms for the In particles in the melt-spun Al-7wt% In sample

(a) and the ball-milled Al-7 wt% In sample, at a heating rate of 10°C/min

(b) The reference curve is the melting DSC curve for the “bulk” In in the as-cast In/Al alloy. T_e is the equilibrium melting temperature of pure In^[39-41]

4.2 Hardness

Two nonequilibrium processes (melt-spinning and ball-milling) were successfully employed to synthesize $\text{Al}_{1-x}\text{Pb}_x$ ($x=5\text{wt}\%$, $10\text{wt}\%$, $20\text{wt}\%$, $30\text{wt}\%$) nanocomposites with distinct microstructures. In the meltspun(MS) Al-Pb alloys, the nanometer-sized Pb particles are uniformly distributed in the

micrometer-grained Al matrix and have an orientational relationship with the matrix. While in the ball-milled (BM) samples, both Pb and Al components are refined with prolonged milling time, forming nanocomposites with Pb particles homogeneously dispersed into the Al matrix. The microhardness of the BM Al-Pb samples is much larger than that of the MS samples, which mainly results from strengthening effects of the nanometer scale Al grains following the Hall-Petch relationship as shown in Fig 12.^[43]

5 Conclusions

(1) There has an abrupt temperature rise during mechanical alloying due to the high heat of formation of compound from elemental powders.

(2) Amorphization or local melting may be happened under appropriate conditions.

(3) Mechanical alloying is an important technology to produce metastable phases, and influences the structure and mechanical properties.

(4) There have some differences of the formation products produced by mechanical alloying and rapid quenching, such as melting point and hardness.

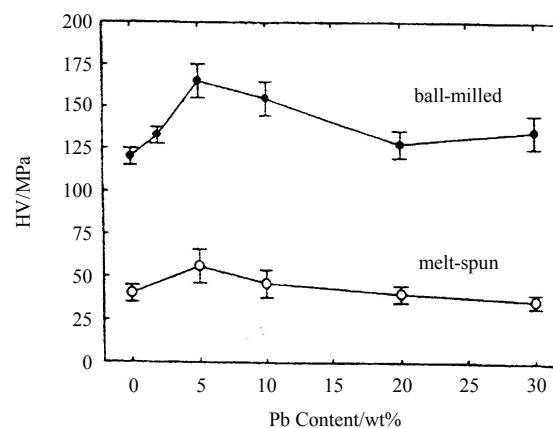


Fig. 12 Microhardness of the Al-pb powders for MS $Al_{1-x}Pb_x$ (open circle) and BM $Al_{1-x}Pb_x$ samples milled for 10h (closed circle) as a function of the content of Pb^[43]

References

- [1] Benjamin J S. Metall. Trans., 1970, Al: 294
- [2] Koch C C, Cavin O B, McKamey C G, Scarbrough J O. Appl. Phys. Lett., 1983, 43: 1017
- [3] Schwarz R B, Petrich R R, Saw C K. J. Non-Cryst. Solids, 1985, 76: 281
- [4] Hellstern E, Schultz L. Appl. Phys. Lett., 1986, 48: 124
- [5] Weeber A W, van der Meer K, Bakker H, de Boer F R, Thijsse B J, Jongste J F, J. Phys F: Met. Phys., 1986, 16: 1897

- [6] Koch C C, Mater. Sci. Forum, 1992, 88~90: 243
- [7] Yermakov A Y, Yurchikov Y Y, Barinov V A. Fiz. Met. Metalloved., 1981, 52: 50
- [8] Schwarz R B, Koch C C. Appl. Phys. Lett., 1986, 49: 146
- [9] Ye L L, Liu Z G, Li S D, Quan M X, Hu Z Q. J.Mater. Res., 1997, 12: 616
- [10] Fan G J, Song X P, Quan M X, Hu Z Q. Scripta Mater., 1996, 35: 1065
- [11] Lou T P, Fan G J, Ding B Z, Hu Z Q. J. Mater. Res., 1997, 10: 1172
- [12] Liu Z G, Ye L L, Guo J T, Li G S, Hu Z Q. J.Mater. Res., 1995, 10: 3129
- [13] Liu Z G, Guo J T, Ye L L, Li G S, Hu Z Q. Appl. Phys. Lett., 1994, 65: 2666
- [14] Liu Z G, Guo J T, Hu Z Q. Mater. Sci. Eng., 1995, A192/193: 577
- [15] Liu Z G, Guo J T, He L L, Hu Z Q. Nanostr. Mater., 1994, 4: 787
- [16] Liu Z G, Guo J T, Li G S, Hu Z Q. Acta Metall. Sin., 1994, 7: 7
- [17] Ye L L, Huang J Y, Liu Z G, Quan M X, Hu Z Q. J.Mater. Res., 1996, 11: 2092
- [18] Sheng H W, Xu J, Yu L G, Sun X K, Hu Z Q, Lu K. J.Mater. Res., 1996, 11: 2841
- [19] Sheng H W, Zhao Y H, Hu Z Q, Lu K. Phys. Rev. B, 1997, 56: 2302
- [20] Sheng H W, Xu J, Sun X K, Lu K, Hu Z Q. Nanostr. Mater., 1995, 6: 417
- [21] Ye L L, Liu Z G, Huang J Y, Quan M X. Mater. Lett., 1995, 25: 117
- [22] Fan G J, Guo F Q, Hu Z Q, Quan M X, Lu K. Phys. Rev. B, 1997, 55: 11010
- [23] Lou T P, Ding B Z, Gu X J, Li G S, Hu Z Q. Mater. Lett., 1996, 28: 129
- [24] Yavari A R, Desre P J, Benameur T. Phys. Rev. Lett., 1992, 68: 2235
- [25] Hellstern E, Fecht H J, Fu Z, Johnson W L. J.Appl. Phys., 1989, 65: 305
- [26] Koch C C. Nanostr. Mater., 1993, 2: 109
- [27] Eckert J, Schultz L, Urban K. Appl. Phys. Lett., 1989, 55: 117
- [28] Fan G J, Quan M X, Hu Z Q. Scripta Metall. Mater., 1995, 33: 377
- [29] Liu Z G, Guo J T, Hu Z Q. J. Alloys and Comp., 1996, 234: 106
- [30] Fan G J, Song X P, Quan M X, Hu Z Q. Mater. Sci. Eng., 1997, A231: 111
- [31] Fan G J, Gao W N, Quan M X, Hu Z Q. Mater. Lett., 1995, 23: 33
- [32] Fan G J, Quan M X, Hu Z Q. J.Mater. Sci. Lett., 1995, 14: 523
- [33] Fan G J, Quan M X, Hu Z Q, Shin K S, Yoon J K, Kim S J. Proc. of the 2nd Pacific Rim Intern. Conf. on Adv. Mater. and Processing. The Korean Institute of Metals and Materials, 1995. 2133
- [34] Fan G J, Quan M X, Hu Z Q. Scripta Metall. Mater., 1995, 32: 247
- [35] Ye L L, Quan M X, Shin K S, Yoon J K, Kim S J. Proc. of the 2nd Pacific Rim Intern. Conf. on Adv. Mater. and Processing. The Korean Institute of Metals and Materials, 1995. 2143
- [36] Liu Z G, Guo J T, Shi N L, Hu Z Q. J.Mater. Sci. Technol., 1996, 12: 7
- [37] Ye L L, Liu Z G, Quan M X, Hu Z Q. J.Appl. Phys., 1996, 80: 1910
- [38] Fan G J, Quan M X, Hu Z Q. Appl. Phys. Lett., 1996, 68: 319
- [39] Sheng H W, Ren G, Peng L M, Hu Z Q, Lu K. J.Mater. Res., 1997, 12: 1
- [40] Sheng H W, Ren G, Peng L M, Hu Z Q, Lu K. Phil. Mag. Lett., 1996, 73: 179
- [41] Sheng H W, Ren G, Peng L M, Hu Z Q, Lu K. J.Mater. Res., 1997, 12: 119
- [42] Sheng H W, Hu Z Q, Lu K. Nanostructured Mater., 1997, 9: 661
- [43] Sheng H W, Zhou F, Hu Z Q, Lu K. J.Mater. Res., 1998, 13: 308